Journal of Nuclear Materials 394 (2009) 52–62

Contents lists available at ScienceDirect

Journal of Nuclear Materials

journal homepage: www.elsevier.com/locate/jnucmat

Effect of pH on corrosion behavior of CuCrZr in solution without and with NaCl

C.T. Kwok [a], P.K. Wong [a], H.C. Man [b], F.T. Cheng [c,*]

[a] Department of Electromechanical Engineering, University of Macau, China
[b] Department of Industrial and Systems Engineering, The Hong Kong Polytechnic University, Hong Kong, China
[c] Department of Applied Physics, The Hong Kong Polytechnic University, Hong Kong, China

ARTICLE INFO

Article history:
Received 23 June 2009
Accepted 1 August 2009

ABSTRACT

CuCrZr is a high copper alloy widely used as electrical and thermal conducting material, especially in heat exchangers in nuclear reactors. In this respect, the physical and fatigue properties of CuCrZr have been extensively studied. The electrochemical behavior of CuCrZr, on the other hand, has not been adequately investigated. In the present study, the effect of pH on the corrosion behavior of CuCrZr in aqueous solutions without and with chloride (0.6 M NaCl) was studied. The pH of the solutions is found to exert significant influence on the corrosion behavior of CuCrZr. In acidic solutions without chloride, the corrosion of CuCrZr is ascribed to active dissolution with soluble products. In neutral and alkaline solutions without NaCl, the presence of oxides on the surface of CuCrZr leads to a noble shift in corrosion potential and passivation results in increased corrosion resistance. In chloride solutions at various pH values, the chloride ions influence the formation of the surface layers and the anodic dissolution process during polarization. At high pH, CuCrZr shows significant passivity and high corrosion resistance due to the growth of Cu_2O/Cu(OH) film which hinders further dissolution whereas at low pH the corrosion resistance is lowered due to active dissolution of Cu.

1. Introduction

High copper alloy CuCrZr is age-hardenable, beryllium-free and dilutely alloyed with Cr and Zr. Its advantages include excellent electrical and thermal conductivities, high strength, ease of fabrication, high fatigue resistance and radiation resistance, and low toxicity. Through age-hardening, the mechanical and tribological properties of the alloy can be enhanced while high levels of electrical conductivity can be preserved [1]. CuCrZr has extensive applications such as overhead contact wires for electric railway, electrodes and holders for welding, electrical components working under mechanical stress and spark, lead frame for integrated circuit, moulds and dies for continuous casting metals, and heat sinks for nuclear power reactors. The applications of CuCrZr may involve acidic, alkaline and chloride-containing environments. Although copper is a noble metal, it reacts readily in oxygen-containing environment, with the anodic dissolution of copper electrochemically balanced by oxygen reduction [2,3]. It was reported that the corrosion rate of copper is influenced by the pH and has the lowest value in slightly alkaline solutions. The corrosion of CuCrZr in adverse working conditions, for instance, in polluted atmosphere and in nuclear reactors with different water chemistries [4], is critical for determining the lifetime and reliability of the engineering components.

In the literature, some studies were focused on the dealloying of copper alloys with high content of Cr [5,6] and Zr [7]. It is found that dechromisation of Cu–47%Cr [5] and Cu–50.54%Cr–0.42%Ni–1.34%Al [6] in acidic media occurs at the interface between the Cr-rich phase and the Cu-rich phase, and gradually extends to the Cr-rich phase until Cr is completely dissolved. Lu and his coworkers studied the corrosion behavior of the Cu–Zr alloys with 15%, 30%, and 66% of Zr in 0.1 M HCl [7]. The results revealed that Cu–15%Zr has the highest corrosion resistance in the potential region of selective dissolution of Zr while the Zr content has little effect on the selective dissolution rate of Zr when it is above 30%. On the other hand, report on the corrosion behavior of high copper alloys micro-alloyed with Cr and Zr is scarce. Zhang and his coworkers reported the effect of chloride concentration (0.01–1 M) on the corrosion behavior of CuCr, CuZr and CuCrZr [1]. Significant reduction in corrosion resistance was observed with simultaneous micro-addition of Cr and Zr, compared with addition of Cr or Zr alone. It was also shown that the element Zr plays a deteriorating role to the Cu_2O layer while Cr plays an offsetting role [1]. In these reports [1,5–7], the effect of pH on the corrosion behavior of CuCrZr has not been studied, though CuCrZr could be exposed to environments with different pH values.

The aim of the present work is to investigate the effect of pH on the corrosion behavior of high copper alloy CuCrZr compared with

* Corresponding author. Tel.: +852 2766 5691; fax: +852 2333 7629.
E-mail address: apaftche@polyu.edu.hk (F.T. Cheng).

0022-3115/$ - see front matter © 2009 Elsevier B.V. All rights reserved.
doi:10.1016/j.jnucmat.2009.08.006

Table 1
Designation, compositions and hardness of pure copper and various copper alloys.

Designation	UNS number	Hardness (Hv)	Composition (in wt%)		
			Cu	Cr	Zr
Cu	C11000	102.0	Bal.	–	–
CuCrZr	C18150	168.8	Bal.	1.4	0.12
CuCr	C18200	162.5	Bal.	1.2	–
CuZr	C15000	132.8	Bal.	–	0.25

Cu, CuCr and CuZr in solution without and with 0.6 M NaCl by open-circuit potential measurement and potentiodynamic polarization. In addition, the morphology of the corroded surface was also investigated.

2. Experimental details

Wrought cylindrical bars of precipitation-hardened high copper alloy CuCrZr (C18150) was selected for the present study. Annealed

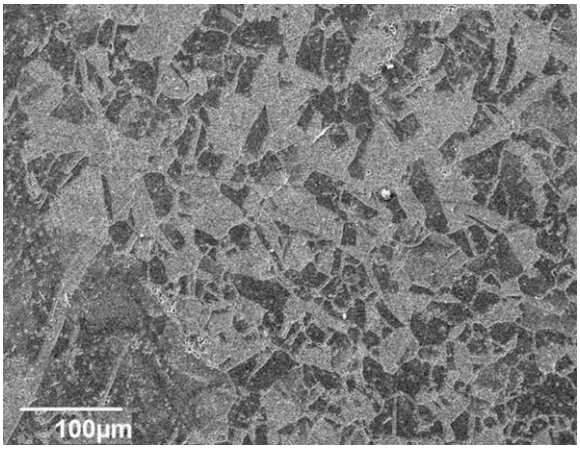

Fig. 1. SEM micrograph of CuCrZr.

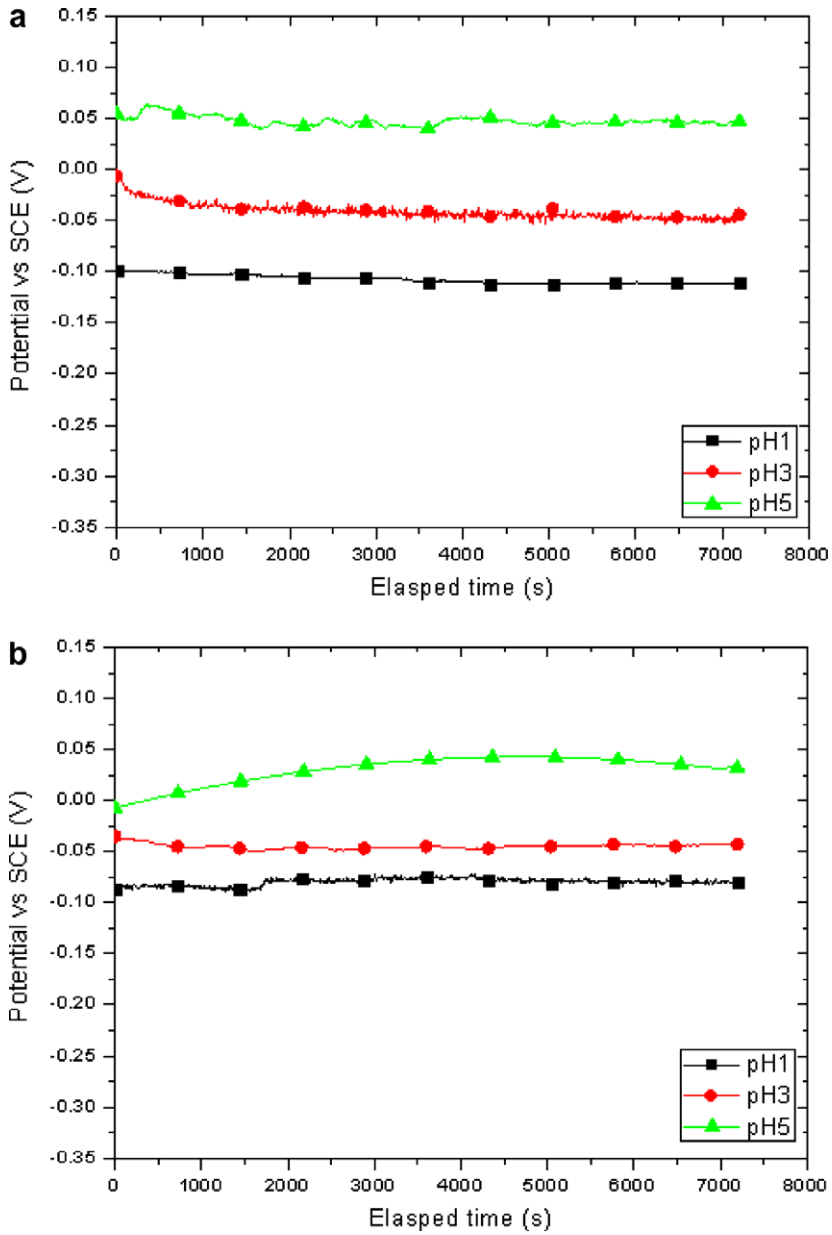

Fig. 2. Plots of OCP vs time for (a) CuCrZr and (b) Cu in solutions pH 1, 3, 5 without NaCl.

Cu (C11000) and precipitation-hardened CuCr (C18200) and CuZr (C15000) were included for comparison purpose and for exploring the role of the alloying elements on the corrosion behavior of the alloys. Disc specimens of diameter of 13 mm and thickness of 10 mm were prepared by a cut-off machine with coolant. The Vickers hardness of the specimens was determined using a microhardness tester at a load of 200 g and a loading time of 10 s. The designation, chemical compositions, and Vickers hardness of the tested specimens are shown in Table 1. Prior to the corrosion tests, the specimens were mechanically ground by CAMI 800-grit silicon carbide paper, degreased in alcohol, rinsed in distilled water, and finally dried in a cool air stream.

To investigate electrochemical corrosion behavior, the specimens were embedded in cold-curing epoxy resin. Epoxy resin was also applied at the interface between the specimens and the mount in order to avoid crevice corrosion as well as to expose a test area of 1 cm^2. In order to avoid the influence due to air exposure, the test solutions were freshly prepared by dissolving 35 g NaCl in 965 ml distilled water and the pH was varied by adding H_2SO_4 or NaOH. Open-circuit potential (OCP) measurement and potentiodynamic polarization test in the freshly prepared solutions without and with 0.6 M NaCl at pH values of 1, 3, 5, 7, 10 and 12, open to air at 25 ± 1 °C, were performed in a three-electrode cell in a water bath using a PAR VersastatII potentiostat according to ASTM Standard G5-94 [8]. All potentials were measured with respect to a saturated calomel electrode (SCE, 0.244 V versus SHE at 25 °C) as the reference electrode. Two parallel graphite rods served as the counter electrode for current measurement. After the OCP measurement for a period of 2 h, the final steady OCP was recorded and then the potential was increased at a rate of 1 mV s^{-1}, starting from 0.2 V below the OCP and terminated at 1 V. From the polarization curves, the corrosion current densities (I_{corr}) of the alloys in various test conditions were determined by fitting to the linear region using Tafel extrapolation with the aid

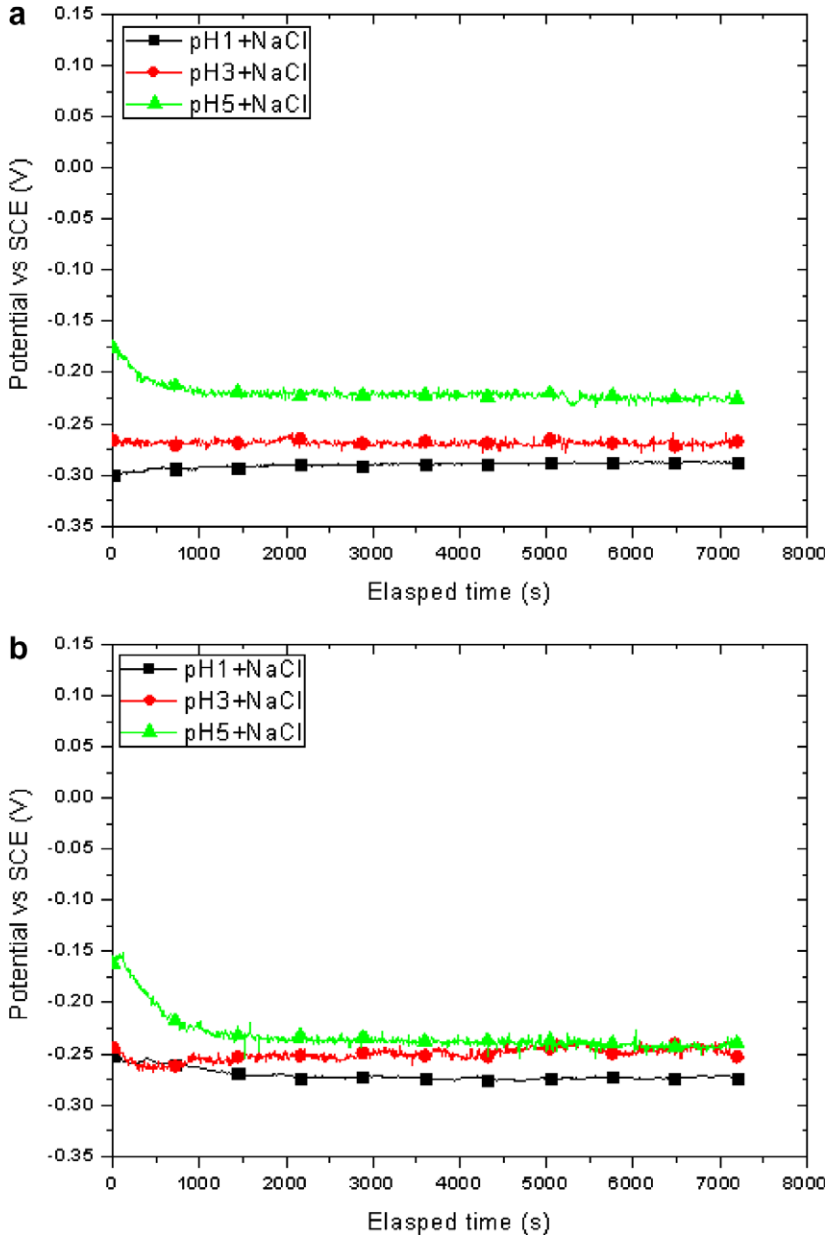

Fig. 3. Plots of OCP vs time for (a) CuCrZr and (b) Cu in solutions pH 1, 3, 5 with NaCl.

of commercial software (PowerCORR, V.2.42). For specimens showing pitting corrosion behavior at high pH, the pitting potentials and passive currents were also recorded.

The microstructure, morphology of the corroded surface, and chemical composition of the corrosion products of CuCrZr were investigated by scanning-electron microscopy (SEM, Hitachi S-3400N) and energy dispersive X-ray spectroscopy (EDX, Horiba EX-250).

3. Results and discussion

3.1. Microstructure

The microstructure of CuCrZr consists of equiaxed, twinned grains of alpha copper solid solution as shown in Fig. 1. Typically it had been cooled rapidly so the Cr and Zr remained in solid solution. The precipitation treatment allowed the Cr and Zr to precipitate out of the solid solution, forming a dispersion of Cr and Zr precipitates throughout the matrix. The precipitates of Cr and Zr are too fine and invisible at low magnification.

3.2. Open-circuit potential measurements

The plots of OCP against time for CuCrZr and Cu in solutions at various pH without and with chloride are shown in Figs. 2–5. The steady values are summarized in Table 2 and plotted against the pH values as shown Fig. 6. In general, the OCPs for CuCrZr and Cu in 0.6 M NaCl solution are more active than those in the solutions without chloride. For CuCrZr in 0.6 M NaCl solution, the OCP peaks at pH 7 while in solutions without NaCl, the OCP peaks at pH 5 (Fig. 6a). On the other hand, the OCP of Cu in 0.6 M NaCl solution increases monotonically with pH in the range pH 1–12, while in solution without NaCl, the OCP peaks at pH 5 (Fig. 6b).

The Pourbaix diagrams for Cu, Cr and Zr in water at 25 °C shown in Fig. 7 provide a thermodynamic basis for explaining the phenomena of dissolution and oxide formation in aqueous solutions

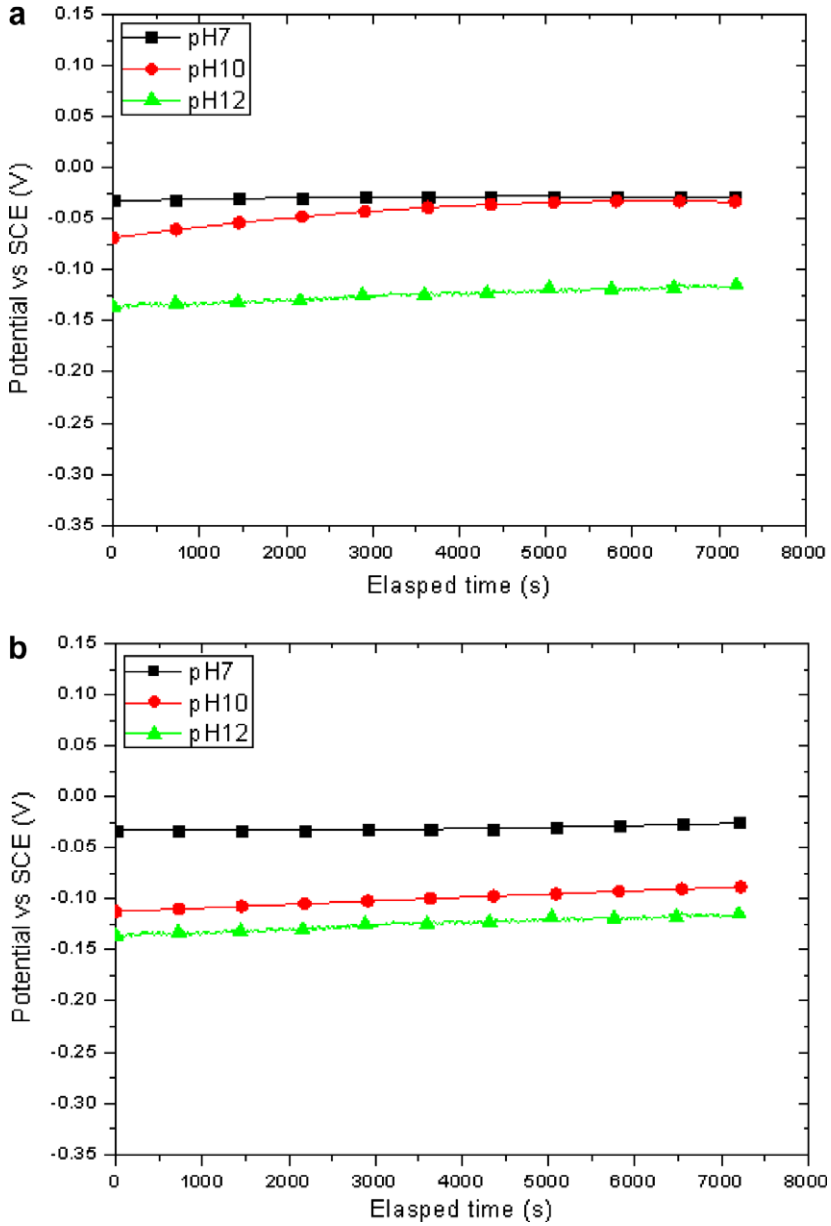

Fig. 4. Plots of OCP vs time for (a) CuCrZr and (b) Cu in solutions pH 7, 10, 12 without NaCl.

under different electrochemical conditions [9]. Among these elements, Cu is the noblest but it dissolves as Cu^{+}/Cu^{2+} in acidic solution and oxidizes to $Cu_2O/CuO/Cu(OH)_2$ in neutral and alkaline solutions in aerated oxidizing conditions. Cr shows corrosion resistance by passivity due to the presence of protective oxide which is stable at pH values above 3. Zr corrodes in acidic (pH < 3.5) and alkaline (pH > 13) solutions and the area of oxide stability lies between pH 3.5 and 13. Zr has the lowest redox potential which indicates a large chemical driving force for corrosion. If passivation does not intervene, Zr will react violently with the surrounding chemical species such as chloride, oxygen and water and be converted to its ionic form. Compared with Cu, the difference in standard electrode potentials of Cr and Zr in acidic medium is quite large. From Fig. 7b and c, the immunity region for Cr and Zr is located at lower potential regions. When the applied anodic potential is between the redox potentials of $Zr/Zr^{3+}/ZrO^{2+}$, $Cr/Cr^{2+}/Cr^{3+}$ and $Cu/Cu^{+}/Cu^{2+}$, the dissolution is attributed to the preferential removal of Cr or Zr atoms in the alloys at low pH. The preferential dissolution of Cr/Zr atoms may take place accompanied with hydrogen evolution due to their high electroactivity:

$$Cr + H_2O + H^{+} \rightarrow Cr^{2+} + H_2 + OH^{-} \quad (1)$$

$$Zr + H_2O + 2H^{+} \rightarrow ZrO^{2+} + 2H_2 \quad (2)$$

When selective dissolution occurs, the topmost layer of the alloy surface is depleted of the active elements (Cr or Zr), and preferentially enriched in the more noble element (Cu). Dealloying is largely dependent on the difference between the electrode potentials of the major constituent elements, atomic percent composition and on the kinetics of the solid-state diffusion of the alloyed elements [10]. Although CuCrZr contains a small amount of Cr and Zr (lower than 1.5 wt%), dealloying of CuCrZr still occurs at low pH as a result of the selective dissolution of Cr and Zr according to the Pourbaix diagrams. Alloys containing Zr are expected to be more susceptible to dealloying than the alloys containing Cr because of the larger difference in electrode potentials. The Pourbaix diagrams can provide

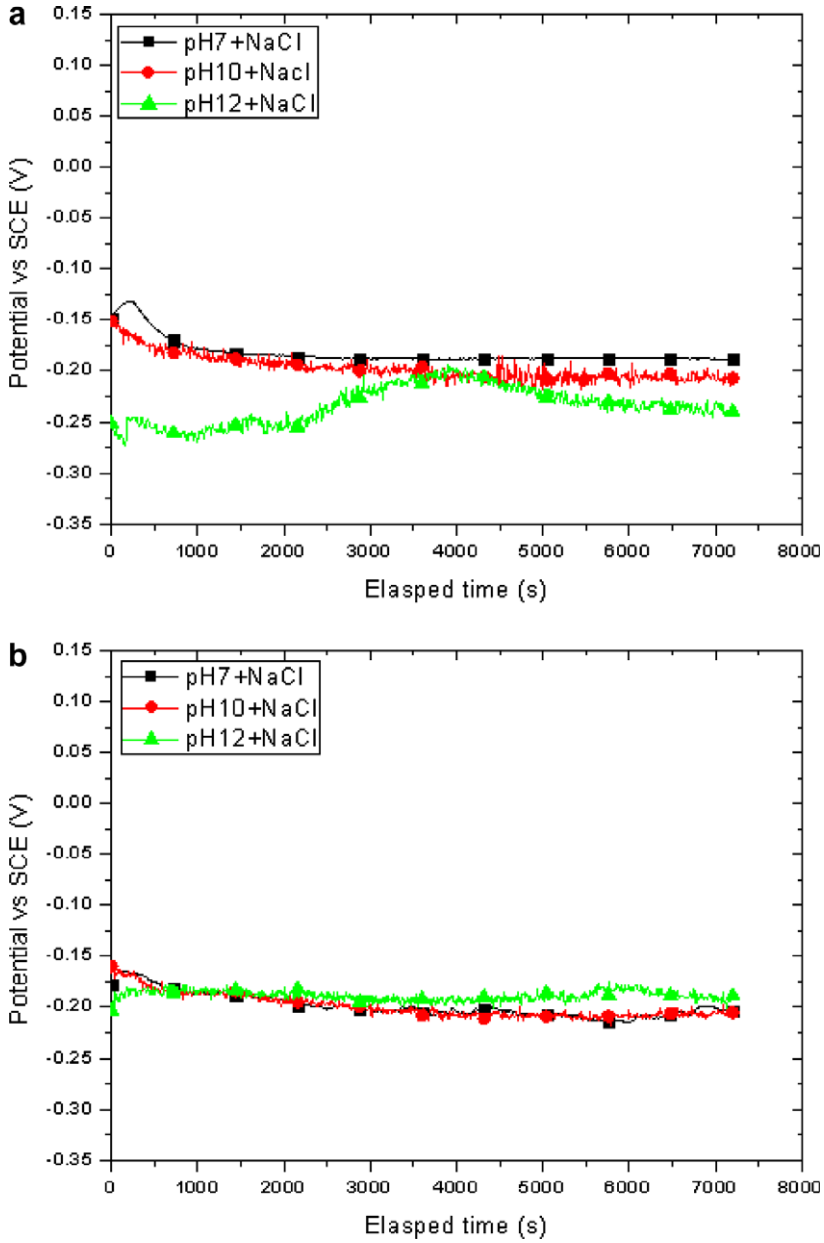

Fig. 5. Plots of OCP vs time for (a) CuCrZr and (b) Cu in solutions pH 7, 10, 12 with NaCl.

Table 2
Corrosion parameters of pure copper and high copper alloys in the solutions at various pH without and with NaCl.

	Without NaCl				0.6 M NaCl			
	OCP (V)	I_{corr} (μA/cm^2)	E_{pit} (V)	I_{pass} (μA/cm^2)	*OCP* (V)	I_{corr} (A/cm^2)	E_{pit} (V)	I_{pass} (μA/cm^2)
CuCrZr								
pH 1	−0.11	0.046	–	–	−0.29	2.025	–	–
pH 3	−0.05	0.084	–	–	−0.27	0.420	–	–
pH 5	0.05	0.034	–	–	−0.23	0.139	–	–
pH 7	−0.05	0.039	0.18	–	−0.19	0.043	–	–
pH 10	−0.04	0.058	0.25	1.7	−0.21	0.121	–	–
pH 12	−0.12	0.131	0.50	10.0	−0.24	0.129	0.53	20
Cu								
pH 1	−0.08	0.295	–	–	−0.27	0.980	–	–
pH 3	−0.04	0.209	–	–	−0.25	0.304	–	–
pH 5	0.05	0.040	–	–	−0.24	0.414	–	–
pH 7	−0.03	0.023	0.13	–	−0.20	0.025	–	–
pH 10	−0.11	0.087	0.15	3.1	−0.20	0.130	–	–
pH 12	−0.12	0.159	0.70	4.2	−0.19	0.227	0.55	20
CuCr								
pH 1	–	–	–	–	−0.22	0.202	–	–
pH 12	–	–	–	–	−0.16	0.271	0.50	20
CuZr								
pH 1	–	–	–	–	−0.23	0.152	–	–
pH 12	–	–	–	–	−0.17	0.243	−0.04	10

information for the thermodynamics of metal dissolution in aqueous environment but the information about the dissolution kinetics will be discussed based on the potentiodynamic polarization behavior of CuCrZr in the next section.

3.3. Polarization behavior at pH 1–5

The potentiodynamic polarization curves of CuCrZr and Cu in acidic solutions without and with chloride NaCl (pH 1, 3 and 5) are showed in Figs. 8 and 9, respectively, and the values of I_{corr} are listed in Table 2. In solutions without and with chloride, the anodic current density and I_{corr} increase and the corrosion potential decreases with increase in acidity. In solutions at pH 3–5 without chloride, a narrow linear portion in the anodic region is observed. The linear region is attributed to diffusion of copper ions in oxide films. In the chloride solutions at pH 1–5, no clear anodic Tafel region and no active–passive transition is observed, showing that anodic dissolution is not in an activation regime. Formation of stable surface oxides is impossible and dissolution of copper is dominant. Feng et al. reported that the oxide film tends to dissolve in acidic solution and the film thickness decreases rapidly when the pH value is lower than 4 [11]. In acidic solutions without chloride, the main anodic reaction that takes place is active dissolution of Cu to Cu^+ at the corrosion potential:

$$Cu \rightarrow Cu^+ + e^- \quad (3)$$

The reaction rate is determined by the cathodic reduction of oxygen in acidic solution:

$$O_2 + 4H^+ + 4e^- \rightarrow 2H_2O \quad (4)$$

Combining (3) and (4),

$$4Cu + O_2 + 4H^+ \rightarrow 4Cu^+ + 2H_2O \quad (5)$$

In solution with chloride ions, the potential of the cathodic–anodic transition region is shifted in the active direction. Higher I_{corr} (i.e. corrosion rates) are recorded and peaks of anodic current density are also observed. When the applied anodic potential is higher than the dissolution potential of Cu, dissolution of Cu occurs through the mass-transfer controlled step in the Tafel region [12]. The initial reaction is the formation of less soluble CuCl solid [13]:

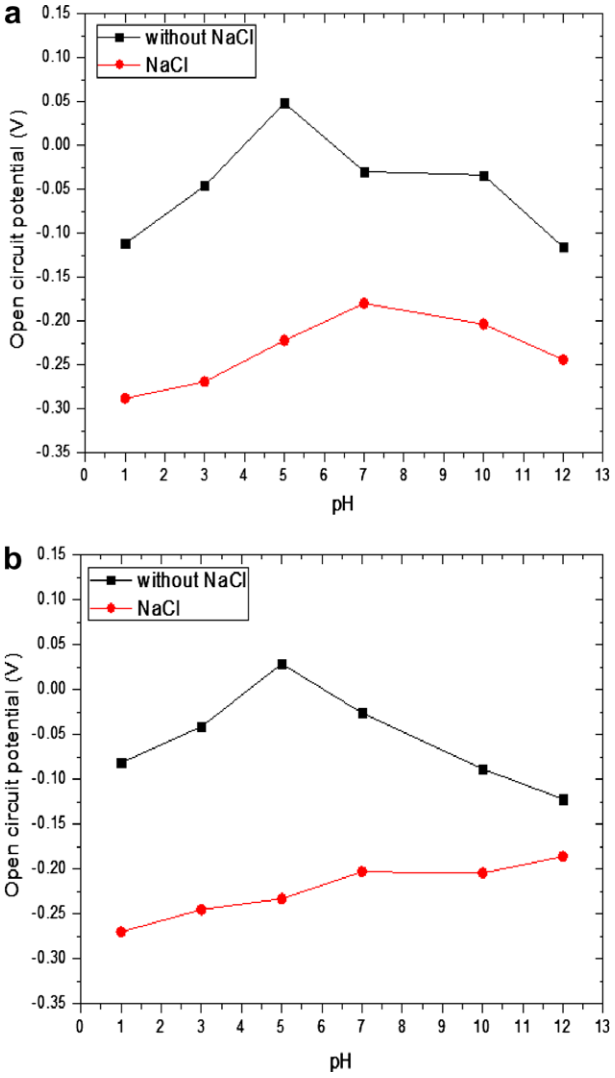

Fig. 6. Effect of pH on OCP of (a) CuCrZr and (b) Cu in solutions without and with 0.6 M NaCl.

$$Cu + Cl^- \rightarrow CuCl_{(s)} + e^- \quad (6)$$

Moreover, copper oxidizes to cuprous chloride complexes and the rate is dependent on chloride concentration but independent of pH [14].

Cuprous ions can diffuse through solid-state CuCl until they meet with chloride ions, and then the following reaction takes place:

$$Cu^+ + Cl^- \rightarrow CuCl_{(s)} \quad (7)$$

As the potential is further increased, the anodic curves exhibit small peaks due to the formation of CuCl film at a potential of about −0.05 V. At chloride concentrations higher than 0.3 M (0.6 M in the present study), the insoluble CuCl layer transforms into a soluble $CuCl_2^-$ complex [1] and then $CuCl_2^-$ hydrolyzes to form a passive Cu_2O layer and so a decrease in the corrosion rate can be observed.

3.4. Polarization behavior at pH 7–12

The potentiodynamic polarization curves of the CuCrZr and Cu in the near-neutral solution (pH 7) and alkaline solutions (pH 10 and 12) with and without NaCl are shown in Figs. 10 and 11, respectively, and the corrosion parameters are extracted and summarized in Table 2.

In solution without chloride at pH 7, passivation-like behavior is observed in CuCrZr and Cu at higher anodic potentials. However, they do not passivate in chloride solution at pH 7. It has been

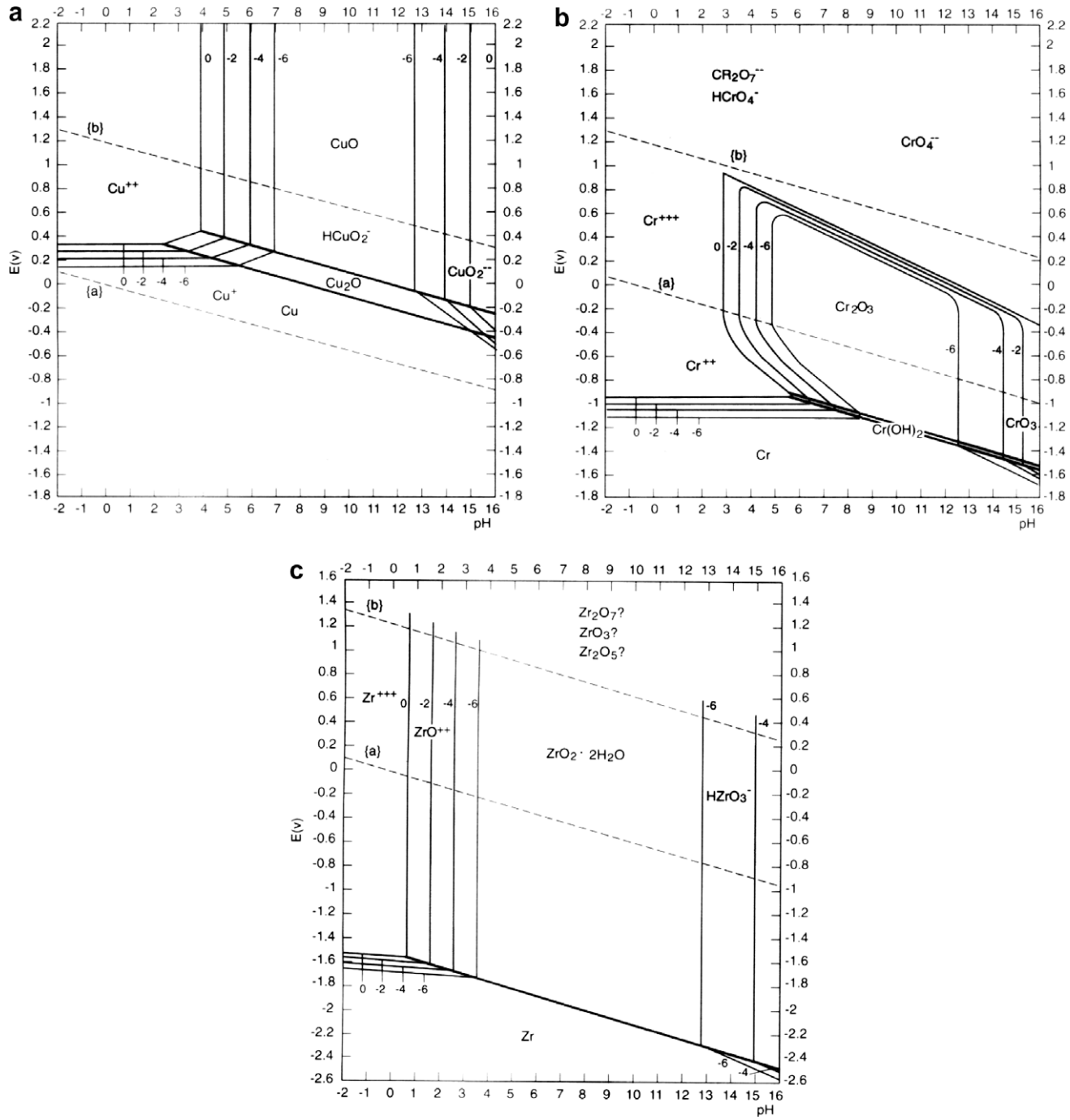

Fig. 7. Pourbaix diagrams for (a) Cu–H_2O, (b) Cr–H_2O and (c) Zr–H_2O systems at 25 °C [9].

reported that the polarization behavior of copper in the Tafel region in chloride solutions is not activation-controlled but is a mass transport-kinetics process; thus dissolution is controlled by the rate of diffusion of $CuCl_2^-$ species from the electrode surface across a diffusion layer whose concentration gradient is determined by the electrode potential [15–17]. As the potential is further increased, the anodic curves exhibit small peaks consistent with the formation of a CuCl film [16,17] at a potential of about −0.05 V. Beyond the peaks, limiting-current behavior is observed and the rate of anodic reaction is controlled by the formation and dissolution of CuCl film [16]. The rate of the reaction is probably determined by the cathodic reduction of oxygen in neutral solution:

$$O_2 + 2H_2O + 4e^- \rightarrow 4(OH)^- \quad (8)$$

In chloride solution at pH 7, the I_{corr} of Cu and CuCrZr are the lowest (Fig. 11). It seems their polarization behaviors in chloride solutions are dominated by the dissolution of copper to soluble cuprous chloride ion complex $CuCl_2^-$.

For CuCrZr in solution without chloride at pH 10, passivation is observed and the passive range (−0.1 to 0.25 V) is wider than that of CuCrZr at pH 7 and Cu at pH 10 (Fig. 10). Their passive current densities are of the order of μA/cm^2. A thin and dense Cu_2O layer formed on the surface of CuCrZr and Cu results in spontaneous passivation. On the other hand, the polarization curves of CuCrZr and Cu show active behavior in chloride solution at pH 10 and are similar to those at pH 7 (Fig. 11). The curves for CuCrZr and Cu in 0.6 M NaCl start with similar active regions followed by active–passive transition that occurs at comparable potentials. The sudden increase of anodic currents at higher potentials is due to film breakdown, being accompanied by corrosion.

It has been shown that the potentiodynamic behavior of copper in slightly alkaline solution exhibits anodic peak associated with the electro-formation of Cu_2O and CuO. Formation of Cu_2O occurs through:

$$2Cu + H_2O \rightarrow Cu_2O + 2H^+ + 2e^- \quad (9)$$

and subsequent oxidation of Cu_2O to CuO film at higher potentials, according to:

$$Cu_2O + H_2O \rightarrow 2CuO + 2H^+ + 2e^- \quad (10)$$

Thus, passivity breakdown at pH 10 occurs with the formation of Cu_2O for CuCrZr at lower potential and with the growth of CuO film for Cu at higher potential. This is attributed primarily to the generation of H^+ ions at the electrode surface [18].

For CuCrZr and Cu in solution without chloride at pH 12, the behavior at the active region appears to be influenced by high alkalinity. The noticeable Tafel region shows a large slope and wide

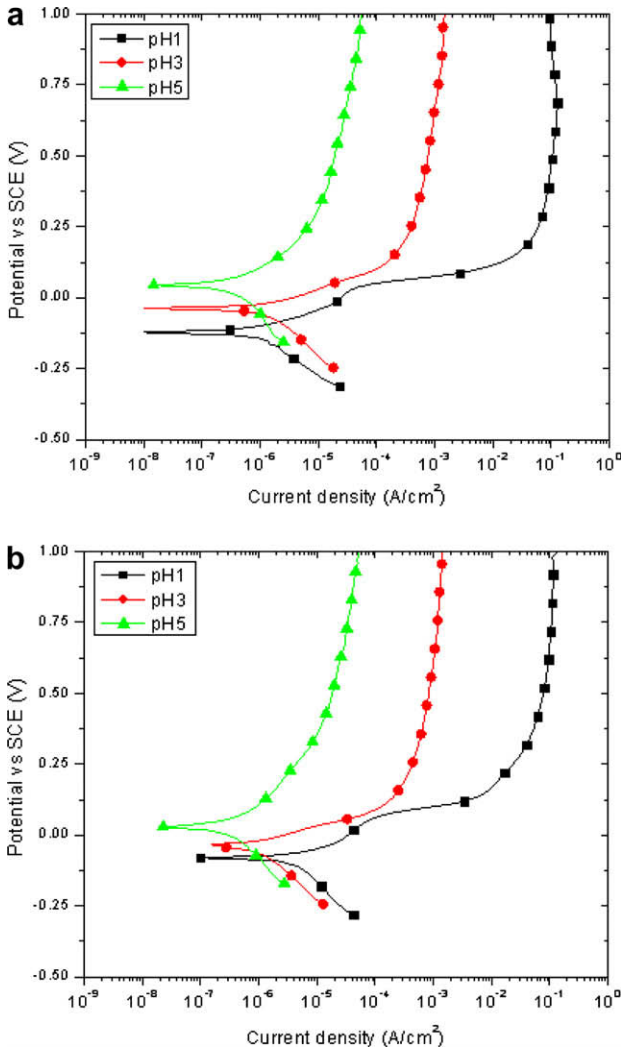

Fig. 8. Potentiodynamic polarization curves of (a) CuCrZr and (b) Cu in acidic solutions (pH 1, 3, 5) without NaCl.

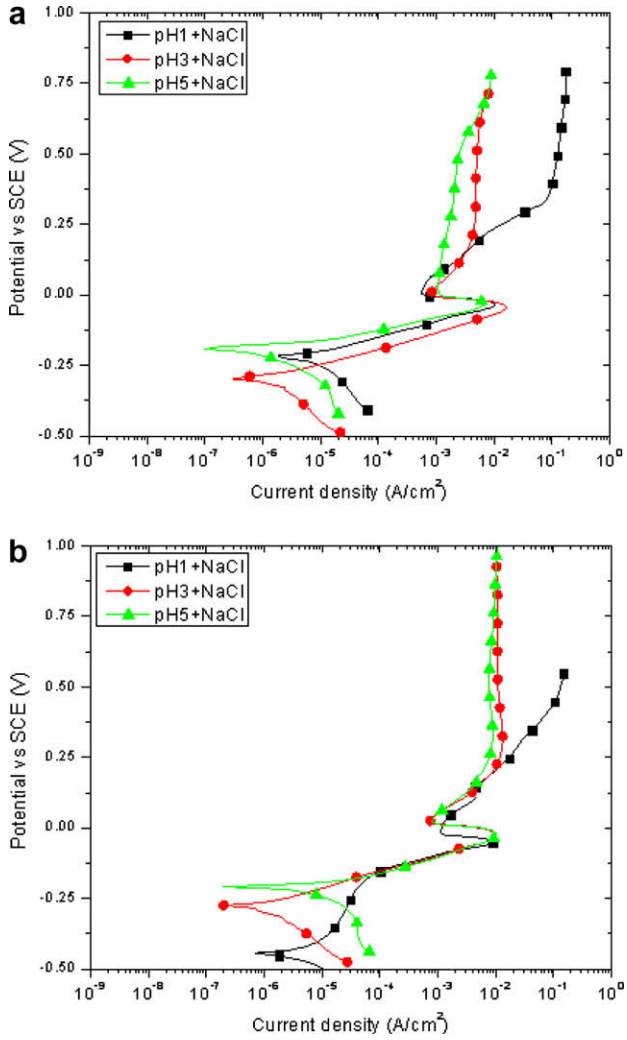

Fig. 9. Potentiodynamic polarization curves of (a) CuCrZr and (b) Cu in acidic solutions (pH 1, 3, 5) with 0.6 M NaCl.

passive range. CuO layer is formed and its thickness increases rapidly due to high alkalinity. The polarization curves (Fig. 10) exhibit a passive region with an anodic peak which corresponds to the formation of $Cu(OH)/Cu_2O$ layer [19,20] through the following reactions:

$$2Cu + 2OH^- \rightarrow Cu_2O + H_2O + 2e^- \quad (11)$$

and subsequent oxidation of Cu_2O to $Cu(OH)_2$ film at higher potentials, according to:

$$Cu_2O + 2OH^- + H_2O \rightarrow Cu(OH)_2 + 2e^- \quad (12)$$

In chloride solution, the film stability of CuCrZr and Cu is lower but the curves still exhibit wide passive ranges (Fig. 11). As the potential is increased above the pitting potential, breakdown becomes evident. The polarization curves show two passive regions with two anodic peaks. The first peak corresponds to the formation of the $Cu(OH)/Cu_2O$ layer. The second peak is more complex and involves the formation of $Cu(OH)/Cu_2O$ and $Cu(OH)_2/CuO$ [21].

3.5. Effect of pH on I_{corr}

The plots of corrosion rates (reflected by I_{corr}) against the pH value of the solutions are shown in Fig. 12. The corrosion rates of CuCrZr and Cu are the highest in chloride solution at pH 1 and lowest at pH 7. Dissolution of oxide films takes place when the pH is lower than 5. Between pH 7 and 10, Cu_2O film is formed and the film is not so protective. When pH is greater than 10, CuO film starts to form and excellent passivity is observed.

3.6. Effect of Cr and Zr on corrosion behavior

The polarization curves of CuCrZr and Cu are compared with those of CuCr and CuZr in chloride solutions at extreme pH values (1 and 12) as shown in Fig. 13. The anodic current densities of CuCrZr, CuCr, CuZr and Cu at pH 1 do not vary much due to active dissolution of Cu. On the contrary, at pH 12, Cu, CuCrZr and CuCr exhibit a wide passive range and high pitting potentials ($\geqslant$0.5 V) whereas CuZr shows very narrow passive range and localized film breakdown occurs at relative low anodic potential (−0.04 V). The addition of the more active Zr deteriorates the corrosion resistance of CuZr significantly at pH 12. Zhang and his coworkers reported that Zr plays a deteriorating role to the Cu_2O layer while Cr plays an offsetting role in 1 M NaCl neutral solution [1]. In the binary alloys (CuCr and CuZr), the effect of the element Zr is markedly stronger than that of Cr in chloride solution at pH 12. However, no significant reduction in pitting corrosion resistance is observed when both Cr and Zr are present in CuCrZr. It is may be attributed to its lower Zr content (0.12 wt%) compared with CuZr (0.25 wt%).

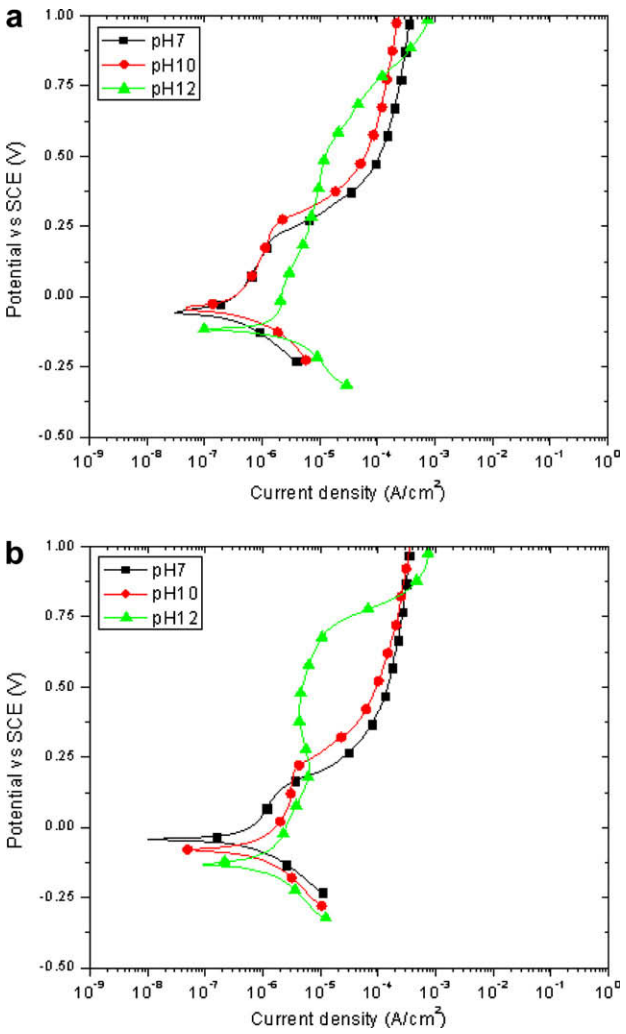

Fig. 10. Potentiodynamic polarization curves of (a) CuCrZr and (b) Cu in neutral and alkaline solutions (pH 7, 10, 12) without NaCl.

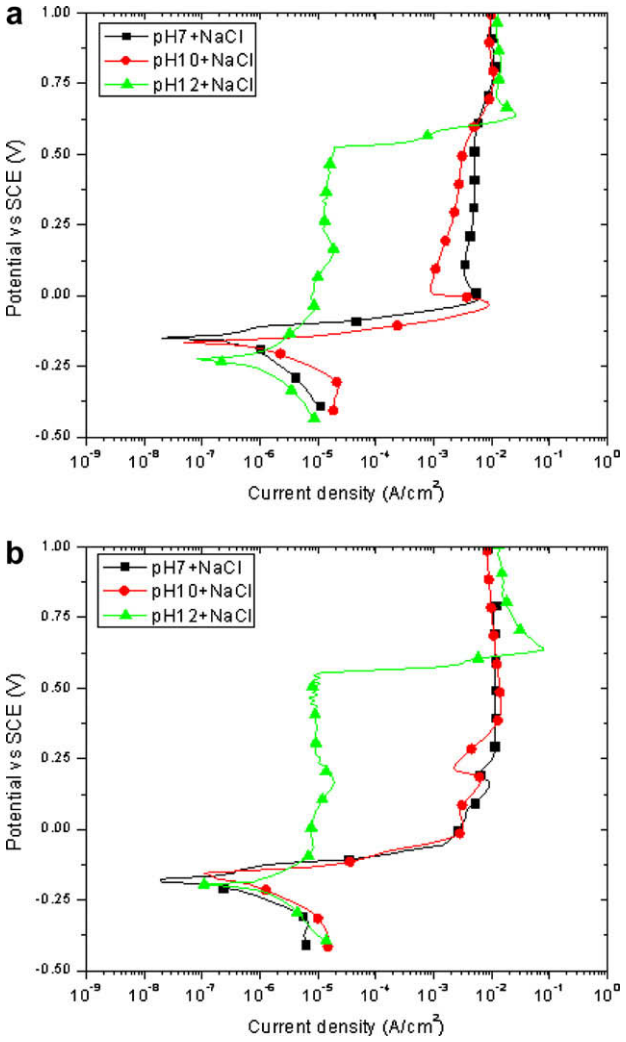

Fig. 11. Potentiodynamic polarization curves of (a) CuCrZr and (b) Cu in neutral and alkaline solutions (pH 7, 10, 12) with 0.6 M NaCl.

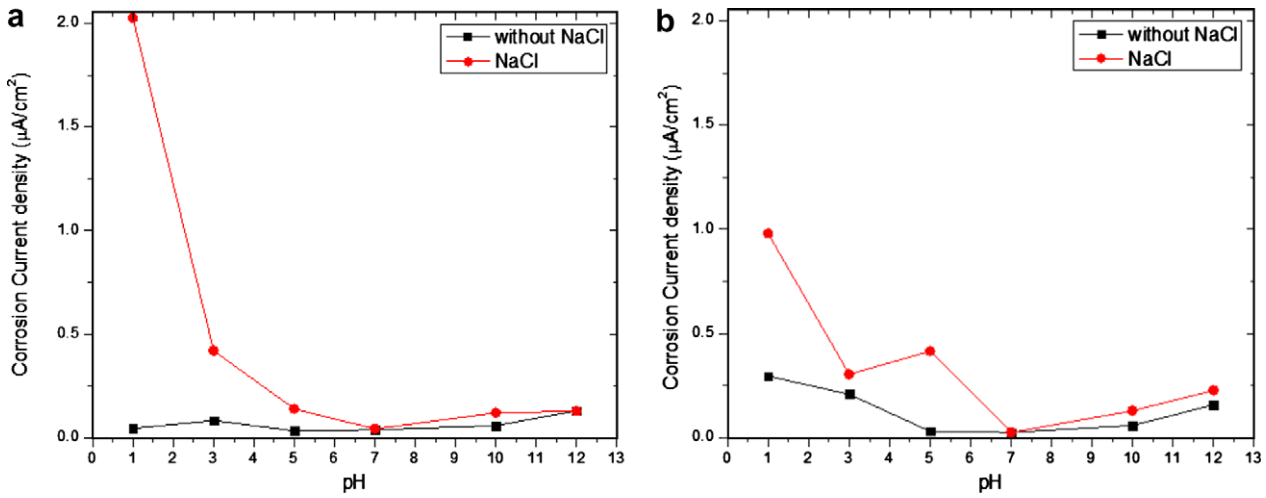

Fig. 12. Effect of pH on I_{corr} of (a) CuCrZr and (b) Cu in solutions at various pH without and with chloride.

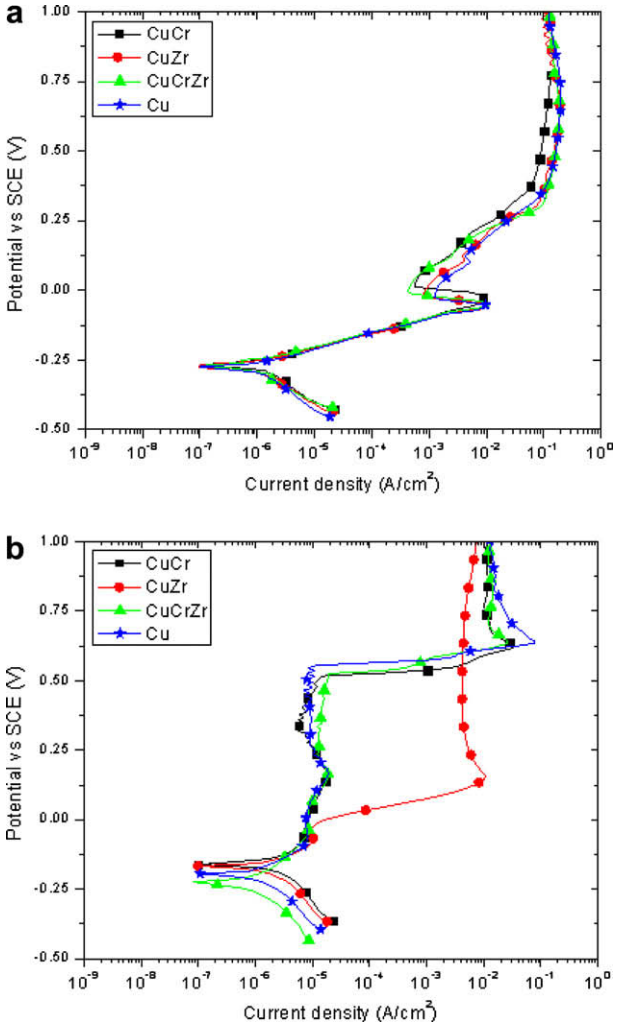

Fig. 13. Potentiodynamic polarization curves of various copper alloys in 0.6 M NaCl solution at (a) pH 1 and (b) pH 12.

Based on the value of E_{pit}, the pitting corrosion resistance of the alloys is ranked as:

$$CuZr \ll CuCr \sim CuCrZr < Cu$$

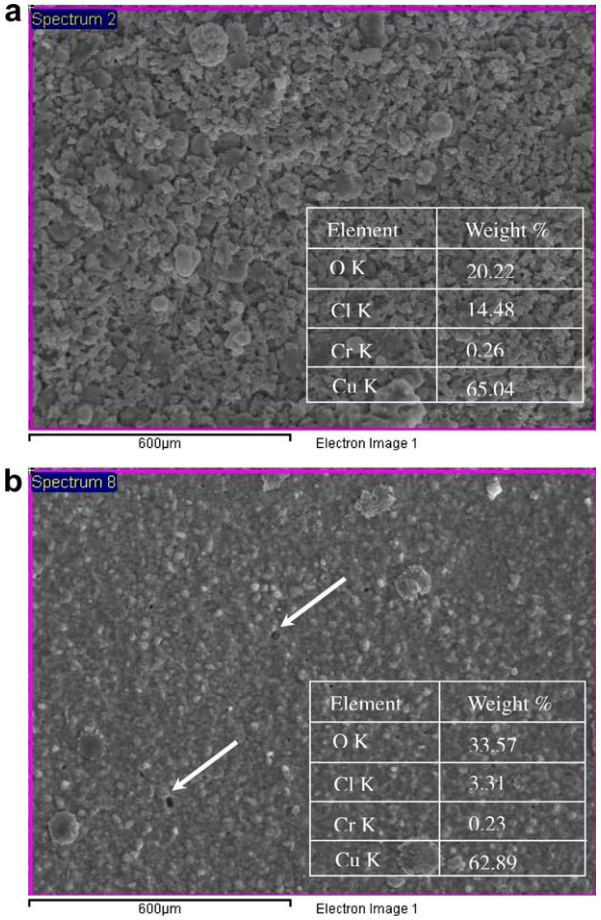

Fig. 14. SEM and EDX analyses of corrosion product for CuCrZr in chloride solution at (a) pH 1 and (b) pH 12 after polarization tests.

Among the alloys investigated, Cu has the highest pitting corrosion resistance at pH 12.

3.7. SEM and EDX analyses

The SEM micrographs of corroded CuCrZr in chloride solutions at pH 1 and 12 with EDX spectra of the corrosion products are

shown in Fig. 14. SEM examinations of CuCrZr corroded in chloride solution at pH 1 reveal uniform corrosion with corrosion products covering the entire surface (Fig. 14a). Small discrete pits are observed for CuCrZr corroded in chloride solution at pH 12 as shown by the arrows in Fig. 14b. It is observed that the degree of corrosion damage is more severe in CuCrZr in chloride solution at pH 1. EDX results of the corroded surface of CuCrZr in chloride solution at pH 1 contains relatively high Cl and O with a tiny amount of Cr. It is likely that the corrosion product consists mainly of copper chlorides. On the other hand, the corroded surface of CuCrZr in chloride solution at pH 12 contains more O, and the corrosion product consists mainly of copper oxides. In addition, some $Cr(OH)_2$ or Cr_2O_3 could also be formed.

4. Conclusions

1. The open-circuit potentials for CuCrZr and Cu in 0.6 M NaCl solution are more active than those in solutions without chloride.
2. The open-circuit potentials for CuCrZr and Cu shift in the active direction as acidity increases due to active dissolution, independent of the presence of chloride.
3. The corrosion rates (reflected by I_{corr}) of CuCrZr and Cu are the highest in NaCl solution at pH 1 and the lowest at pH 7.
4. The corrosion rates (reflected by I_{corr}) of CuCrZr, Cu, CuCr and CuZr at pH 1 do not differ significantly as at this low pH corrosion is controlled by active dissolution of Cu.
5. On the contrary, at pH 12, CuCrZr, Cu, and CuCr exhibit significant passivity and high pitting potentials ($\geqslant 0.5$ V) whereas CuZr shows very narrow passive range and localized film breakdown occurs at relative low anodic potential (-0.04 V).

Acknowledgements

The work described in this paper was fully supported by a research grant from the Fundo para o Desenvolvimento das Ciencias e da Tecnologia (FDCT 018/2008/A) and the Research Committee of University of Macau (Project No. RG064/07-08S/KCT/FST). Support from the infrastructure of University of Macau and the Hong Kong Polytechnic University is also acknowledged.

References

[1] Y.N. Zhang, J.L. Zi, M.S. Zheng, J.W. Zhu, J. Alloys Compd. 462 (2008) 240.
[2] M. Metikos-Hukovic, R. Babic, I. Paic, J. Appl. Electrochem. 30 (2000) 617.
[3] Y. Feng, K.S. Siow, W.K. Teo, K.L. Tan, A.K. Hseih, Corrosion 53 (1997) 389.
[4] V. Belous, G. Kalinin, P. Lorenzetto, S. Velikhopolskiy, J. Nucl. Mater. 258–263 (1998) 351.
[5] T. Xu, L. Chen, Y. Chen, S.X. Yu, B. Liu, J.H. Liu, Trans. Nonferrous Met. Soc. China 14 (2004) 520.
[6] C.Y. Yu, L.M. Chang, L.M. Zhou, H.Y. Lin, Trans. Nonferrous Met. Soc. China 16 (2006) 229.
[7] H.B. Lu, Y. Li, F.H. Wang, Electrochim. Acta 52 (2006) 474.
[8] ASTM G5 – 94 (2004) Standard Reference Test Method for Making Potentiostatic and Potentiodynamic Anodic Polarization Measurements, ASTM Standards, ASTM, Philadelphia, PA, USA.
[9] D.A. Jones, Principles and Prevention of Corrosion, second ed., Prentice-Hall, NJ, 1996. pp. 62–63.
[10] B.G. Ateya, H.W. Pickering, Corros. Sci. 38 (1996) 1245.
[11] Y. Feng, W.K. Teo, K.S. Siow, G.L. Tan, A.K. Hseih, Corrosion 53 (1997) 389.
[12] H.P. Lee, K. Nobe, J. Electrochem. Soc. 133 (1986) 2035.
[13] L. Stephenson, J.H. Bartlett, J. Electrochem. Soc. 101 (1954) 571.
[14] H.P. Lee, K. Nobe, A.J. Pearlstein, J. Electrochem. Soc. 132 (1985) 1031.
[15] A.L. Bacarella, J.C. Griess, J. Electrochem. Soc. 120 (1973) 459.
[16] D. Tromans, J.C. Silva, Corrosion 53 (1997) 171.
[17] D. Tromans, R. Sun, J. Electrochem. Soc. 138 (1991) 3235.
[18] D. Tromans, R. Sun, J. Electrochem. Soc. 139 (1992) 1945.
[19] M.R. Gennero de Chialvo, S.L. Marchiano, A.J. Arvia, J. Appl. Electrochem. 14 (1984) 165.
[20] J.G. Beccera, R.C. Salvarezza, A.J. Arvia, Electrochim. Acta 33 (1988) 613.
[21] H. Wojtas, H. Boehni, Mater. Sci. Eng. A 134 (1991) 1065.